Available online at www.sciencedirect.com

ScienceDirect

Focus Article, *Mendeleev Commun.*, 2021, **31**, 137–148

Mendeleev Communications

Preparation, chemical features, structure and applications of membrane materials based on graphene oxide

Dmitrii I. Petukhov,*[a,b] Olesya O. Kapitanova,[a,b,c] Elena A. Eremina[b] and Eugene A. Goodilin[a,b]

[a] *Department of Materials Science, M. V. Lomonosov Moscow State University, 119991 Moscow, Russian Federation. E-mail: di.petukhov@gmail.com*

[b] *Department of Chemistry, M. V. Lomonosov Moscow State University, 119991 Moscow, Russian Federation*

[c] *Center for Photonics and 2D Materials, Moscow Institute of Physics and Technology, 141701 Dolgoprudny, Moscow Region, Russian Federation*

DOI: 10.1016/j.mencom.2021.03.001

Emerging chemical techniques for preparation of modern 2D materials lead inevitably to broadening the areas of practical applications on demand of the materials. One of the most bright trends in research and development of the most famous 2D material, graphene oxide, involves the search for optimal mass production, optimization and flexible adjustment of membrane materials for various practical needs as always based on unique structural and chemical features of graphene oxide itself. Here, physical chemical correlations between preparation history, structural peculiarities of graphene oxide and functional properties of graphene oxide-based membranes are reviewed and analyzed.

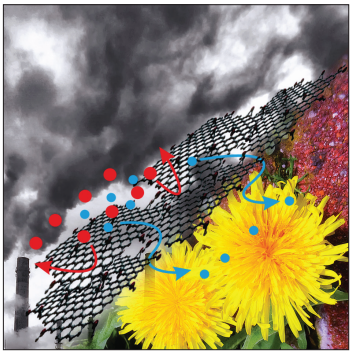

Keywords: graphene oxide, membranes, gas separation, pervaporation, water desalination.

Introduction

The Nobel Prize in Physics in 2010 and the discovery of graphene followed by innovative experiments with this new two-dimensional form of 'sp^2 carbon' ('nanocarbon') initiated a spectacular rise of fundamental researches and practical implementations of all two-dimensional materials.[1] One of the most bright trends in research and development of the most famous 2D material, graphene oxide (GO), involves the search for optimal mass production, optimization and flexible adjustment of membrane materials for various practical needs. Involvement of 2D materials for the control of separation processes in the field of membrane science and membrane

Dmitrii I. Petukhov obtained BC, MS and PhD degrees in chemistry at the Department of Materials Science of the M. V. Lomonosov Moscow State University, currently – a senior research scientist of the Department of Chemistry of the M. V. Lomonosov Moscow State University. The area of his scientific interests is the development of new membrane materials for separation processes in gas and liquid media.

Olesya O. Kapitanova received BC, MS and PhD degrees from the Department of Materials Science, M. V. Lomonosov Moscow State University. In 2010–2015 she had internship at the Quantum-functional Semiconductor Research Center at Dongguk University, Seoul, Korea. She is currently senior research scientist of the Moscow Institute of Physics and Technology and M. V. Lomonosov Moscow State University. Her research interests include the synthesis and characterization of oxide nanomaterials and structures for use in the fabrication of electronic and photonic nanodevices.

Elena A. Eremina, PhD, Associated Professor, Department of Chemistry of the M. V. Lomonosov Moscow State University, scientific secretary of a dissertation council. A known specialist in chemical education. Main research interests are connected with soft chemistry preparation of inorganic materials, nanomaterials, graphene-based nanocomposites.

Eugene A. Goodilin, Dr. Sci., Professor, Department of Materials Science, Department of Chemistry, M. V. Lomonosov Moscow State University. A specialist in inorganic and solid state chemistry. The recent research field and the area of professional interests are related to nanochemistry, various nanomaterials and chemical aspects of their preparation routes, mostly, for chemical power sources, solar cell batteries, plasmonics and SERS.

technology originates from the pioneering work by Nair *et al.*[2] For the last 8 years, membranes based on different 2D materials, such as graphene and graphene oxide, MXenes, MoS_2, C_3N_4, and other nanosheet materials have been successfully utilized for providing separation processes in both the gas and liquid media.[3,4] Utilization of these membrane materials allows one to purify hydrogen or capture CO_2 with high efficiency. In a liquid phase, these membranes have been effectively utilized for water–alcohol separation by partial water vaporization through the membrane (pervaporation process) or for purifying water away from small organic molecules (nanofiltration) and dissolved inorganic salts (reverse osmosis). Among other 2D materials, graphene oxide has attained closer attention to theoretical and experimental studies due to its extraordinary mechanical strength and chemical stability, diverse chemical nature of functional groups[5–7] and cost-effective synthesis by chemical oxidation, solvent-assisted exfoliation or electrolytic oxidation of graphite.[8,9] The presence of hydrophilic groups makes GO nanosheets easily dispersible in aqueous solutions with the formation of stable suspensions thus that can be utilized for the fabrication of laminar GO membranes by different techniques. A huge progress has been achieved in utilization of GO membranes in gas separation for extraction of small molecules, such as hydrogen and helium,[10] and in the processes based on water molecules penetration through the membrane – reverse osmosis and dehumidification. GO membrane demonstrates NaCl rejection about 97.5% with water permeation 13.7 l m^{-2} bar^{-1} h^{-1},[11] exceeding permeance-rejection characteristics of most existing polymer membranes. Also, GO membranes demonstrate high water vapor permeance up to 80 m^3(STP) m^{-2} bar^{-1} h^{-1} enabling, in combination with a low permanent gas permeance, to achieve H_2O/N_2 selectivity of more than 10 000.[12] At the same time, graphene oxide is a very diverse material both in its chemical composition and microstructure, which, in turn, determine the properties of the formed membranes. Moreover, during the separation process, some GO parameters, such as interlayer distance, may undergo changes under external conditions thus making it possible to suggest 'smart membranes' with a highly controlled permeation mechanism.

In the current review, we focus mainly on preparation of graphene oxide, effective routes of membranes fabrication and the influence of physical chemical properties of GO nanosheets and membrane microstructure on its permeance and selectivity. The limitations and drawbacks of GO membranes preventing their immediate widespread implementation are discussed. A brief overview on the utilization of GO based membranes in different separation processes, like gas separation, pervaporation, and solution desalination, is presented. Finally, this focus article aims to highlight the importance of preparation history, compositional and structural parameters of GO nanosheets and microstructural parameters of membranes for the analysis of substance transport through the membranes and prospects of their practical applications.

Synthesis techniques and chemical features of graphene oxide

The term graphene oxide includes, as usually defined, a wide class of compounds since no narrow and precise definition is yet negotiated. To the contrary to special cases of expensive epitaxial graphene and its derivatives, GO is normally prepared *via* two widely known mass production approaches: bottom-up – by the oxidation of preliminary obtained graphene species and top-down – by oxidation of graphite followed by exfoliation. In each approach, both the chemical nature of oxidizers, oxidation conditions and the type of carbon precursor drastically influence structural and functional properties of such as-formed graphene oxide.

The first approach involves oxidation of graphene monolayers preliminary deposited by a CVD technique or mechanical exfoliation using atomic oxygen,[13] oxygen plasma,[14] ozone,[15] or even ion bombarding followed by an acidic treatment with potassium permanganate.[16] Definitely, this approach often results in state-of-the-art single layer membranes with unique and remarkable parameters, while large scale fabrication of membranes requires cheaper scaled up production of GO nanosheets.

The top-down methods are of key importance for large-scale graphene oxide preparation in which graphite is oxidized and exfoliated chemically (ChGO) and/or electrochemically (EcGO). The chemical synthesis is based on graphite exposure to strong oxidizing agents, such as a mixture of concentrated nitric acid and potassium chlorate (the Brodie method),[17] or a mixture of nitric and sulfuric acids with potassium chlorate (the Staudenmaier method),[18] or a mixture of potassium permanganate, sodium nitrate and concentrated sulfuric acid (the Hummers method).[19] The reaction, as well known, involves intercalation of molecules and ions from the oxidizing mixture into the interlayer space of graphite, causing gradual oxidation of the graphite matrix, followed by exfoliation into monolayer flakes. Since the oxidation disrupts the graphite's aromatic structure, it accompanied by either transition of carbon atoms from the sp^2- to the sp^3-hybridized state or essential deformation of the flat carbon grids. Atomic carbon to oxygen ratio (C : O) for ChGO varies typically from 1.7 to 3, depending on the preparation conditions. The C : O ratio is experimentally controlled by oxidant quantity variation in the graphite oxidation process[20,21] or post-treatment oxidation[22] or reduction.[23] Also, the chemical origin of termination groups is assumed as another important characteristic of graphene oxide because GO with a similar morphology and oxidation degree obtained by Hummers or Brodie techniques demonstrate quite different distribution of oxygen groups and its relative content.[24,25] For both Hummers-derived GO and Brodie GO, most of the carbon atoms are in the sp^3-hybridization with hydroxyl, epoxy and carbonyl groups on the basal plane of GO and carboxyl groups on the edges of the sheets and on the boundaries of holes. The difference is not significant, however Hummers-derived GO has a higher amount of carbonyl groups and lower amount of hydroxyl groups compared to Brodie-derived GO. Also, Brodie-derived GO demonstrates more uniform distribution of oxygen groups and the lower number of holes in the carbon mesh with respect to Hummers-derived GO. The difference in nanosheets structures and functional groups results expectedly in the divergence of functional properties. Hummers-derived GO samples reveal 3–4 fold increased moisture absorption under ambient conditions (relative humidity ~20–30%) in contrast with Brodie-derived GO. At the same time, membranes based on Brodie-derived GO show more than an order of magnitude higher Young's modulus as compared with Hummers-derived GO.[25] A better flexibility and preparation efficiencies would be achieved using H_3PO_4 as an additional component of the starting oxidizing mixture of potassium permanganate and concentrated sulfuric acid for chemical exfoliation of the graphite. This modification of the Hummers method is known as the Tour method[26] and it allowed one to reduce the number of voids in the graphite structure due to the formation of an intermediate, a relatively stable ether with vicinal diols formed in the course of oxidation of graphite. The C : O ratio and major types of oxygen-containing groups are seen from XPS analysis data with detailed deconvolution of C1s and O1s regions (Figure 1).[27] Also, structural features of graphene oxide are characterized by Raman spectroscopy based on

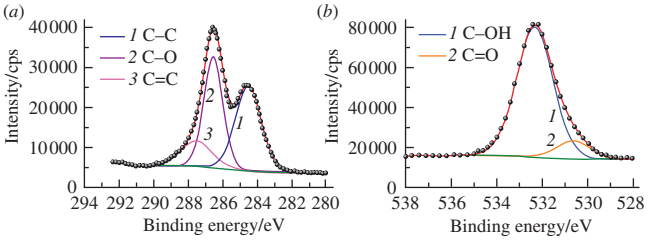

Figure 1 Typical XPS spectra of (*a*) C1s and (*b*) O1s regions of ChGO obtained from thermally expanded graphite as precursors with the C : O ratio of 1.7. Fits of the C1s spectral region were performed using three component lines: C–C (~284.5 eV), C–O (~286.7 eV), C=O (~288.0 eV). Fits of the O1s spectral region were performed using two component lines: C=O (~531.0 eV), C–OH (~532.0 eV).

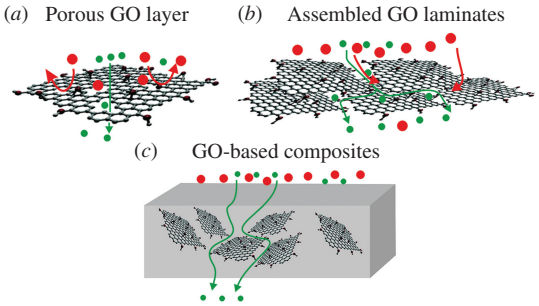

Figure 2 Main types of graphene oxide based membranes: (*a*) single layer membrane, (*b*) few layer membranes and (*c*) composite membrane materials.

analysis of position, intensity and width of D- and G-modes, which, in turn, depends on carbon quantity, bond disorder, clustering of the 'sp^2 phase', the sp^2/sp^3 ratio.[28]

The chemical synthesis parameters allow for varying the lateral size of ChGO particles in a wide range from some (small sheets) to hundreds (large sheets) of microns.[29] The average size of the formed graphene oxide nanosheets depends on carbon precursor used and the GO post-treatment applied. The use of preliminary expanded graphite precursor enables to significantly enlarge the size of nanosheets in comparison with non-expanded precursors.[30] According to the suggested thermodynamic model,[31] an increase in graphite interlayer space facilitates penetration of the oxidizer and thus increases the rate of in-plane oxidation. Also, the GO nanosheets size can be controlled by means of an ultrasonic treatment of GO suspension.[32] Another preparation approach is related to electrochemical exfoliation. This approach is also based on the formation of graphite intercalation compounds (GICs) in the first step followed by oxidation and exfoliation of GIC upon electrolysis of the electrolyte.[33] Compared to the 'purely chemical' method, in electrochemical approach no use of strong oxidizing agents is required since it is an electric field that activates the reaction. This leads to overall significant simplification of the GO purification.

It is considered that the electrochemical way would give a more controlled insertion of ions into the graphite and further oxidation. The overall structural and chemical properties of GO (such as the number of layers, the C : O ratio, the lateral size, the number of defects, *etc*.) are tuned by varying available parameters of the electrochemical treatment (the working potential in the potentiostatic mode, the current density in the galvanostatic mode, the type and concentration of electrolyte).[33,34] Thus, electrochemical approach normally makes it possible to produce larger GO sheets with low defect content and a tunable level of oxidation compared to chemical routes avoiding harsh chemicals and resulting in simplification of product purification. Compared to mechanical exfoliation, molecular assembly and chemical vapor deposition (CVD) methods, the electrochemical approach seems to be more cost-effective for industrial-scale material synthesis thus leading to promising application of membranes while the major part of researches on the formation of graphene oxide membranes still utilizes simple chemical oxidation/exfoliation processes. We conclude here that GO preparation peculiarities predetermines the properties of formed nanosheets such as chemical composition, the average size and the quantity of defects in the carbon mesh. The detailed discussion of synthesis approaches for GO preparation is given elsewhere.[35]

Main types of membrane materials based on graphene oxide

The structural level of molecular scale defects seems to be critically important, however the properties of graphene oxide based membranes depend strongly on the stacking options, which, in turn, depends on the membrane preparation techniques. Basically, nanosheet based membranes can be distinguished into three types based on their microstructure: single layer nanosheet membranes, stacked laminates, and composite membranes filled with nanosheets (Figure 2). The main features of the mentioned membranes are discussed below.

Single layer membranes

A single layer of graphene oxide with a tunable size of defect nanosheets would be assumed as an ideal separation membrane. The size and charge exclusion effects allow one to control the selectivity of such membranes, and the atomic thickness provides the ultimate substance flux of 2 or 3 order of magnitude higher compared with existing membranes.[36] Despite different approaches for defect creation in graphene oxide, discussed early, preferential attention in the literature is paid to both theoretical and experimental studies of single layer graphene membranes. The detailed analysis of gas and ion permeation through the defects in single layer graphene was documented.[37] The study of separation processes using single layer GO membranes is more complicated because of graphene oxide complex structure. Molecular dynamic simulation of the desalination and gas purification performance of single layer reduced graphene oxide membranes with different oxygen concentrations has been performed.[38] It was demonstrated that controllable reduction of graphene oxide with sufficient oxygen group concentration (25 or 33%) allows for preparing rGO nanosheets with the determined number of defects that reveal water permeance about 650 l m^{-2} bar^{-1} h^{-1} with salt rejection >99%. These results might be considered as perfect characteristics for reverse osmosis membranes for desalination purposes. However, no experimental research dedicated to exploring transport through the single layer GO membrane has been published yet while significant attention is paid in the literature to few-layered stacked graphene oxide membranes.

Few-layered laminated GO membranes

Despite the great potential of single layer membranes, their large-scale fabrication techniques are still under development. At the same time, GO nanosheets production is an easy scalable process,[8] which, in combination with different assembling techniques for the preparation of few-layered GO membranes, makes it possible to fabricate large-area membranes and reduce significantly their cost. These membranes can be prepared in a form of free-standing or supported films.[39] Free-standing membranes are not always suitable for industrial applications due to their low mechanical strength. An increase of thickness does not solve the problem since the membrane permeance falls down. Contrary, the fabrication of supported GO layer on porous supports looks like a prospective approach. The main transport path for these membranes is interlayer galleries between stacked

nanosheets, therefore the interlayer distance in these membranes determines primarily their performance in much the same way as the pore diameter determines the performance of classical membranes. The presence of defects in GO also influences the stacked-layer permeance. Moreover, in reality, grain boundaries, interflake regions, wrinkles and nanosheets packing defects can create additional undesired paths for substance transport.

Mixed matrix membranes

Mixed matrix membranes prepared by adding different nanomaterials into polymers were developed to overcome the tradeoff between the permeability and selectivity of polymeric materials. A diverse chemical structure of graphene oxide, including hydroxyl, carboxyl and epoxy groups, provides covalent or non-covalent interactions with different polymer host materials. This allows for preparing the GO–polymer composite membranes demonstrating breakthrough performance in different separation processes. GO-nanosheets embedded in the polymer matrix might create an additional pathway for carrying over water molecules[40] or specific gases.[41] Another possible way of tuning of membrane performance relays on the increase of sorption of specific components by embedded graphene oxide.[42] According to the literature analysis, the fabrication and study of mixed matrix membranes with GO as a filler is a well-discussed topic requiring a separate review. In the current paper, a focus is shifted to the preparation and properties of few-layered graphene oxide membranes.

Preparation of graphene oxide-based membranes

A high nanosheets aspect ratio makes various liquid phase preparation techniques to be effective in the fabrication of free-standing or supported laminar membranes. A given preparation technique determines the thickness, ordering of nanosheets in the formed membranes, a quantity of defects thus providing higher or lower membrane performance. Vacuum- or pressure-driven filtration techniques [Figure 3(*a*)] are widely used to produce laminar GO membranes both as free-standing or supported large-scale films. This process driving force and deposition rate have a strong influence on the microstructure of formed membranes.[43] Utilization of pressure-driven approach allows for producing a uniformly stacked membrane structure due to a nearly constant driving force. Filtration under vacuum leads to the formation of a thin ordered layer with a partial lost of ordering on the external surface of a membrane due to decrease of solvent flux governed by the assemblage of a dense GO layer. Utilization of GO deposition techniques under conditions of solvent evaporation leads to a randomly ordered/disordered microstructure. XRD analysis of the membranes demonstrates that GO-layer *d*-spacing varied from 0.83 nm for membrane prepared *via* pressure-assisted filtration to 1.15 nm for membrane prepared *via* free solvent evaporation. Moreover, the membrane with an ordered laminate structure demonstrates higher water/butanol selectivity in the pervaporation process. The vacuum/pressure-assisted technique is suggested as an easy and scalable process for composite membrane preparation, allowing one to form flat-sheet,[43] tubular, and even hollow fiber membranes.[44] However, the main disadvantages of the above-mentioned technique are time consumption for membrane preparation and a need for thickness control since a thinkable way of thickness tuning utilizes a huge variation of GO suspension concentration from tens to hundreds of mg dm^{-3}.

Different coating (spin-coating, spray-coating, or dip-coating) and casting (drop-casting) processes are suggested as rapid membrane preparation techniques. To improve such coating uniformity and stability of resulting GO membranes, substrates with the opposite charge to GO nanosheets or surface functional groups, that can react with GO nanosheets, are favorable. For this deposition process, the solvent evaporation rate and the deposition speed are key characteristics for the preparation of high-quality membranes. During the spin-coating process [Figure 3(*b*)], an ultrathin laminar GO membrane is formed due to the uniform distribution of GO suspension under centrifugal force. Despite the fact that this approach is suitable only for preparing flat-sheet membranes, it provides about 7 fold growth of permeance characteristics compared to pressure-assisted filtration.[12]

For fast large-scale production of graphene oxide membranes, a spray-coating technique is adopted with large area GO nanofiltration membranes (up to 15×15 cm^2) prepared using this technique [Figure 3(*c*)]. Due to the ultra-thin selective layer

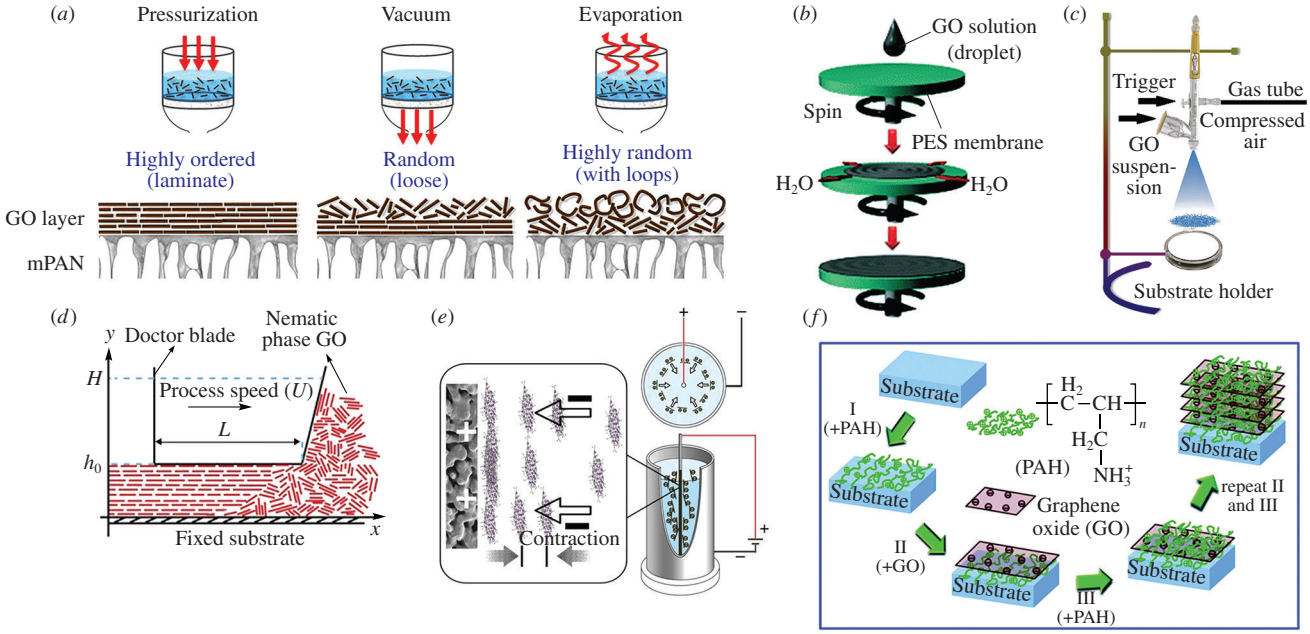

Figure 3 Different techniques for preparation of graphene oxide: (*a*) vacuum/pressure assisted filtration (reproduced from ref. 43 with permission from Elsevier), (*b*) spin-coating technique (reproduced from ref. 47 with permission from the Royal Society of Chemistry), (*c*) spray-coating technique (reproduced from ref. 48 with permission from Elsevier), (*d*) casting technique (reproduced from ref. 46), (*e*) electrophoretic deposition (reproduced from ref. 49) and (*f*) layer-by-layer deposition (reproduced from ref. 50 with permission from the Royal Society of Chemistry).

(<60 nm), the obtained membranes demonstrate high water permeance ~60 l m^{-2} bar^{-1} h^{-1} and high rejection more than 95% for low molecular weight organic dyes owing to dense-packed GO structure.[45] Also, the suggested approach allows for controlling the membrane thickness by varying the number of cycles.

Various casting techniques are adopted for the fabrication of graphene oxide membranes. An example of a known 'doctor blade' technique [Figure 3(*d*)] enables the fabrication of shear-aligned nanofiltration membrane on a large area (13 × 14 cm^2) in less than 5 s.[46] For the resulting membrane, water permeance attains ~70 l m^{-2} bar^{-1} h^{-1} with high retention of organic dye molecules due to a highly ordered structure and low thickness of the GO layer.

A possibility of tuning the GO surface charge and its laminar structure allows one to utilize layer-by-layer preparation techniques. This route makes it possible to adjust membrane thickness at molecular level by varying the number of deposition cycles.[50,51] Because of easiness of deprotonation of functional groups in the GO structure, nanosheets are able to migrate in solution under the electric field to the electrode surface. This enables electrophoretic deposition for membrane preparation on a large area conductive supports.[52] This technique has several advantages – high deposition rate, easy scaling, and the possibility of precise thickness control. However, during the deposition process, partial reduction of graphene oxide often occurs. In some cases, this can improve the membrane selectivity due to the narrowing of the interlayer space,[49] however reduced graphene oxide membranes are moderately applicable to the dehumidification process.

Obviously, a large spectrum of preparation techniques can be utilized to prepare GO membranes both on the lab and industrial scales. The chosen preparation technique is highly important to control the microstructure of the formed membrane, which, in turn, affects the transport properties. The detailed analysis of membrane microstructure is performed using scanning and transmission electron microscopy, Raman intensity mapping.[12]

Influence of microstructure and chemical composition on transport properties of membranes

A typical microstructure of stacked GO membrane is shown schematically in Figure 4. According to the scheme, substances transfer in the ideally packed GO membrane (in this consideration, we will exclude the parasitic transport through the nanosheets stacking defects) through the slit-like pores between GO nanosheets and the defects in GO nanosheets.[53] The size of interlayer space available for substance transport is typically within the range of 0.4–0.9 nm, however the interlayer space can reach several nanometers in the case of swelling in water solutions.[54] The distance between nanosheets defects with a size comparable with gas kinetic diameters is found to be about 10 nm.[55] Due to a high activation energy of molecule penetration through the defects in carbon mesh,[56] the transport through the interlayer galleries seems to be a favorable mechanism.

Gas transport in interlayer galleries when the dimensions of the space available for diffusion is on distances comparable with that of the gas kinetic diameter, is described in terms of activated Knudsen diffusion:[57,58]

$$D_{\text{act.Knudsen}} = \frac{1}{3} h \sqrt{\frac{8RT}{\pi M_r}} \exp\left(-\frac{E_a}{RT}\right), \quad (1)$$

where h is size of the slit available for diffusion, M_r is gas molecular weight, and E_a is activation energy of diffusion. The pre-exponential factor in this equation corresponds to conventional Knudsen diffusion depending only on the pore size.[59] According to published data,[53] the activation energy is close to zero when the ratio $d_{gas}/h < 0.6$ (gas kinetic diameter to slit size). After determination of diffusion coefficient, classical first Fick's law can be used for estimation of membrane permeance. At the same time, stacked packing of GO nanosheets leads to a significant increase in the transport path by factor

$$\frac{L_{av}}{4} \cdot \frac{l}{d_{int}}, \quad (2)$$

where L_{av} is average lateral size of nanosheet, l is thickness of graphene layer, and d_{int} is interlayer distance, and decreases the area available for diffusion by factor h/L_{av}.[60,61]

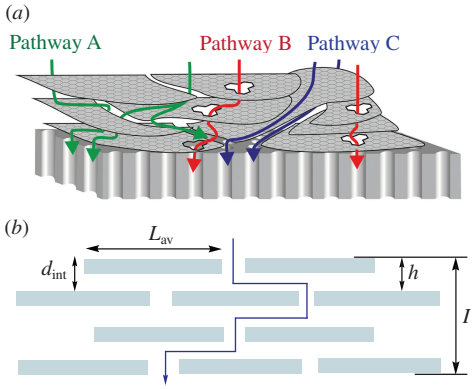

Figure 4 (*a*) Schematic representation of possible transport pathways in GO membranes: diffusion in interlayer galleries (pathway A), transport through the defects in GO nanosheets (pathway B) and parasitic flow through the stacking defects (pathway C) (reproduced from ref. 12 with permission from Elsevier), (*b*) schematic representation of membrane microstructural parameters.

A correct description of a water flow through the stacked GO membranes includes both classical hydrodynamic and molecular dynamic simulations. An application of the classical Hagen–Poiseuille equation, modified for the multilayer structure, gives a suitable description of experimental results for nanofiltration.[62] Simultaneously, a calculation performed using the continuum hydrodynamic approach provides significantly different results in the case of water vapor transport. This difference can be explained by the presence of capillary forces from the evaporative meniscus.[63,64] Effects of nanosheets stacking on the length of water path and available area for water transport have the same influence as discussed above.

From a geometrical point of view, the lateral nanosheet size influences the membrane permeance – an increase of nanosheet size leads to the elongation of transport path. At the same time, the interlayer distance affects the area accessible for diffusion and has a strong influence on the activation energy required for hopping diffusion. Moreover, the value of *d*-spacing determines membrane selectivity due to the size exclusion effect.

Influence of interlayer spacing on the transport properties of membranes

As far as the interlayer distance predetermines strongly the permeance and separation properties of graphene oxide membranes, a large number of techniques are utilized for *d*-spacing analysis like X-ray[65] or neutron diffraction,[66] sorption measurement,[67] or direct measurements of membrane thickness.[68] The operando X-ray diffraction study of water vapor permeance of Hummer-derived GO membrane indicates that water vapor permeance correlates strongly with interlayer spacing, and, in turn, is governed by relative humidity of the reed stream. A decrease of *d*-spacing from 1.05 to 0.95 nm results in water vapor permeance suppressed from 80 to 30 m^3(STP) m^{-2} bar^{-1} h^{-1} followed by diminishing down to negligible values below 0.92 nm [Figure 5(*a*),(*b*)].[64] Graphene

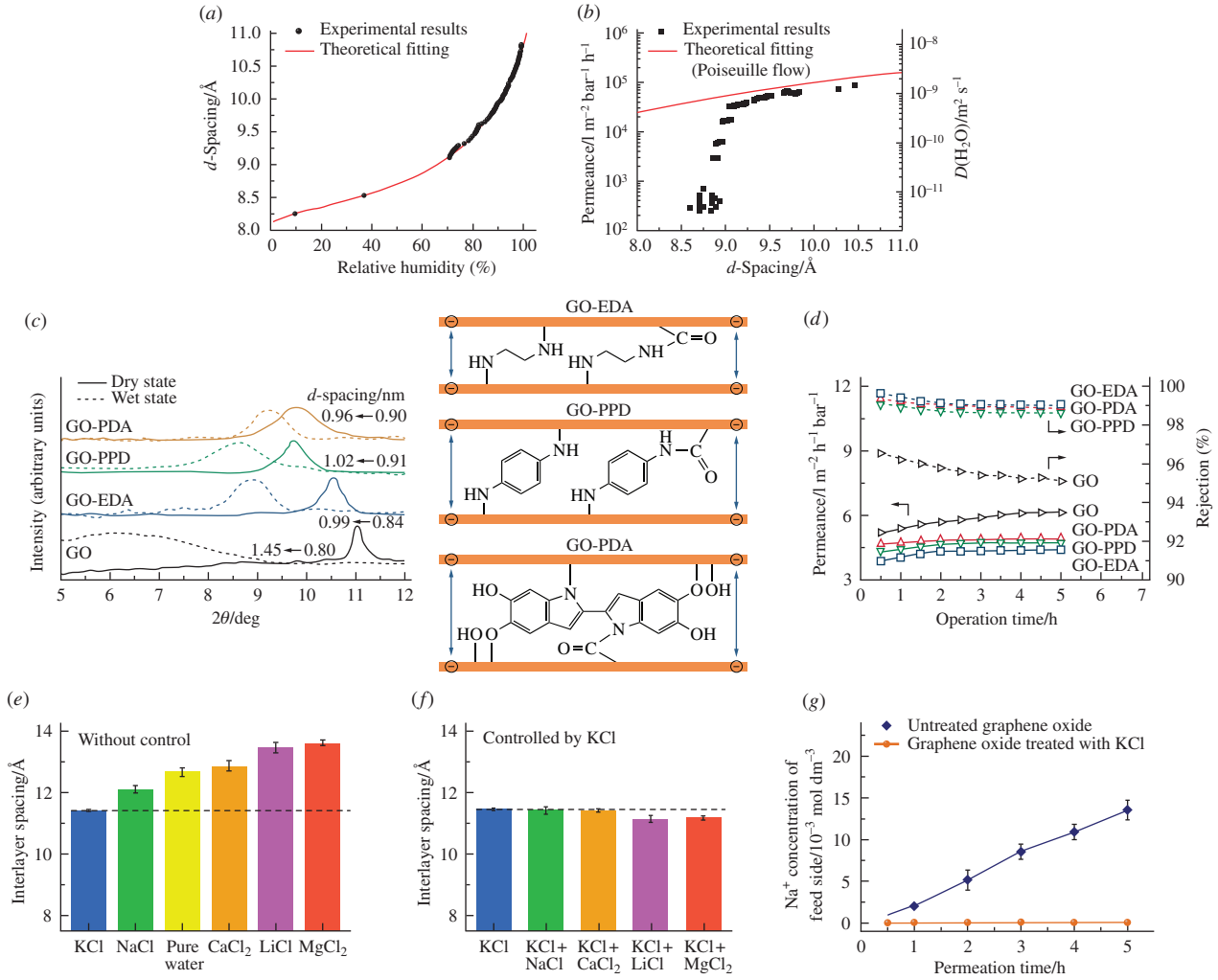

Figure 5 (*a*) Dependence of the interlayer distance in GO membranes *vs*. feed stream relative humidity and (*b*) correlation between water vapor permeance and the GO interlayer distance (reproduced from ref. 64 with permission from IOP). (*c*) Swelling of initial and cross-linked GO membranes in water and (*d*) the results of filtration experiments demonstrating the stability of permeance and rejection characteristics for cross-linked membranes (reproduced from ref. 74 with permission from Wiley). (*e*) The interlayer distance for GO membranes immersed in pure water or in various 0.25 M salt solutions. (*f*) The interlayer distance of GO membranes preliminary soaked in KCl solution and followed immersed in various salt solutions. (*g*) Na^+ permeation rates of untreated GO membranes ($71.84 \pm 6.75 \times 10^{-2}$ mol m^{-2} h^{-1}) and KCl-treated GO membrane ($0.48 \pm 0.07 \times 10^{-2}$ mol m^{-2} h^{-1}) (reproduced from ref. 75 with permission from Springer Nature).

oxide swelling in humid gases is suppressed by an external pressure gradient leading to vapor permeance lost. Simultaneously, the interlayer spacing of GO is stabilized by mixing of GO nanosheets with nanoribbons.[69] Also, the interlayer distance and swelling processes significantly influence the liquid separation processes including pervaporation, forward and reverse osmosis, pressure-driven filtration, *etc*.

An analysis, understanding and controlling of graphene oxide structural features in water–alcohol mixtures are important for predicting the separation properties of these membranes in the pervaporation process. In pure alcohols, the GO interlayer distance depends strongly on the molecule size of absorbed alcohol attaining 2.6 nm for nonan-1-ol due to multilayer absorption.[65] For heavy alcohols, the number of intercalated layers also depends on the ambient temperature and pressure; temperature and pressure decrease leads to an increased intercalated layer, and *vice versa*.[70] Simultaneously, for ethanol and methanol, only one molecular layer can be intercalated between GO nanosheets with the corresponding *d*-spacing of 1.15 and 1.1 nm.[71] The possibility of water molecule multilayer adsorption in the interlayer space of Hummer-derived GO[64] leads to water selective transport in the pervaporation process. To the contrary, the Brodie-derived GO with a more rigid structure demonstrates preferable absorption of methanol molecules from the water–methanol mixture, resulting in the *d*-spacing of about 0.86 nm being lower than that in pure water (1.04 nm).[72] This allows one to fabricate pervaporation membranes with inverse selectivity.

A variation of *d*-spacing with water sorption posts a huge problem for realizing the pressure-driven filtration process with graphene oxide membranes. The hydration phenomena and electrostatic repulsion generated by charged functional groups lead to swelling of GO membranes into aqueous solutions, and such swelling overcomes van der Waals attraction and hydrogen bonds holding nanosheets together, causing disintegration of the membrane.[54,73] Cross-linking of GO nanosheets using different diamines allows for stabilizing the membrane in aqueous solutions. As shown,[74] swelling for 6 h in solution for pristine GO membranes leads to the interlayer distance growth from 0.8 to 1.45 nm associated with a permeance increase by 17% and reduction of rejection of Rhodamine B, as a tracer dye for assessment of filtration efficiency, from 96 to 94%. Simultaneously, GO cross-linking with polydopamine results in stabilization of the membrane since the *d*-spacing changes from 0.9 to 0.96 nm, permeance increases by less than 5%, and no variation of the rejection is observed [Figure 5(*c*),(*d*)]. Moreover, the authors demonstrate the stability of the prepared membrane for 600 h. Besides organic molecules, metal cations are used for

the control of the interlayer spacing to exclude small cations and suppress swelling in water solution. In particular, it is demonstrated that metal cations (K^+, Na^+, Ca^+, Li^+ and Mg^{2+}) precisely tune the interlayer space at one angstrom.[75] Immersion of membrane into KCl solution stabilizes the interlayer distance at about 1.1 nm, leading to the exclusion of other cations [Figure 5(*e*)–(*g*)]. Also, the *d*-spacing of the graphene oxide membrane is narrowed by chemical, thermal[5] or photochemical[76] reduction due to removing, in part, of oxygen-containing groups. Reduction leads to a decrease of the interlayer space down to 0.37–0.4 nm, which is lower than diameters of hydrated sodium (0.716 nm) and chlorine ions (0.664 nm) and it causes significant salt exclusion in the reverse osmosis process.

GO swelling occurs in the vertical direction perpendicular to the nanosheet plane, therefore the external pressure can be used to suppress swelling and reduce the interlayer distance. In particular, application of the external pressure as high as 4 MPa reduces the interlayer distance in the hydrated state down to 0.65 nm, which is lower than the hydrated diameter of potassium ion (0.66 nm).[11]

Despite the detailed analysis of the influence of the interlayer distance on the water transport through GO membranes, the impact of the interlayer distance on gas diffusion is moderately discussed in the literature as explained by the absence of GO swelling effect in a gas phase. GO membranes with the interlayer distance in the range from 0.8 to 0.88 nm (corresponds to slit size 0.5–0.67 nm) have been prepared using spin-coating of solutions with different pH in the range from 3 to 12.[77] No significant variations were observed for hydrogen (kinetic diameter 0.289 nm) and oxygen (0.346 nm); at the same time, growth of the interlayer slit size leads to a two and five fold increase of nitrogen (0.364 nm) and methane (0.384 nm) permeance, respectively. In the work[78], a comparison of gas permeation for Hummers-derived GO membranes with an interlayer distance of 0.86 nm and Brodie-derived GO membranes (0.62 nm) are performed. A decrease of the interlayer space reduces hydrogen and helium permeability in about 3 times whereas methane and carbon dioxide permeability falls down 5 fold and 7 fold, respectively, leading to improved membrane selectivity for industrially important gas pairs H_2/CH_4 and H_2/CO_2. These two works indicate the significant role of activation energy depending on the kinetic diameter to slit size ratio on the gas permeation in confined space between GO nanosheets.

Size of graphene oxide nanosheets

The laminated structure of GO membranes resulted in the diffusion length through the membrane being inversely proportional to the average nanosheet size as shown for gas transport,[53,77] water vapors,[12] and organic solvent nanofiltration.[79] Therefore, improvement of membrane permeance requires the diminishing of the nanosheet lateral size. However, utilization of graphene oxide nanoribbons with their size of 10 nm × 140 ± 20 nm for membrane preparation leads to high porosity and low selectivity towing to the random deposition of ribbons with no resulting laminated structure.[12]

Defects in graphene oxide nanosheets

The possibility of substance transport through defects in graphene oxide nanosheets (pathway B in Figure 4) also influences the permeance of laminated GO membranes. On the one hand, this pathway tortuosity is smaller than the interlayer pathway; on the other hand, the activation energy for molecule penetration through the defect is large and depends on the ratio between the kinetic diameter and the defect size. Pinholes in nanosheet carbon mesh can be fabricated by oxidation of graphene oxide using $KMnO_4$, resulting in an increase of water

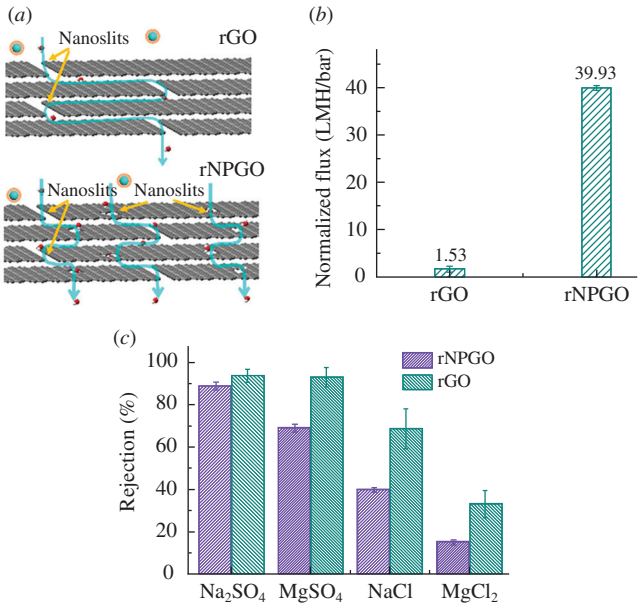

Figure 6 (*a*) Scheme of transport pathways in rGO and nanoporous rGO membranes. Their (*b*) water permeance and (*c*) salt rejection (reproduced from ref. 80).

permeance by a factor of three as compared to the pristine membrane retaining the same rejection.[22] The same technique with following graphene oxide thermal reduction provides the growth of membrane water permeance by a factor of 26 with moderately reducing salt rejection (Figure 6), the declared density of the defect is about 2.89×10^{15} m^{-2} with its average diameter of 3 nm.[80] The authors of ref. 10 explained the high H_2/CO_2 separation factor of the prepared GO membrane by hydrogen transport through the defects in nanosheets, which are impermeable for carbon dioxide. Simultaneously, for elevated temperatures, the pathway B contribution to the transport of large molecules increases.[53] Thus, a controlled process of creation of defects in graphene oxide nanosheets could significantly increase the membrane performance, while this approach is poorly discussed in the literature.

Influence of chemical composition of graphene oxide membranes

The influence of GO chemical composition on the substance transport should not be ignored due to the very diverse chemical nature of graphene oxide prepared by the Hummers, Staudenmainer, or Brodie techniques.[7] Several theoretical works describing gas and water molecules permeation through the graphene oxide membranes possessing different amounts of dominating functional groups are published.[81–84] However, theoretically calculated results might contradict the experimental data, in particular,[83] hydroxyl groups on the graphene oxide suppress water flux because of the effect of a hydrogen bond network. In contrast, the presence of epoxy groups facilitates the water flux increasing. Experimental studies for graphene oxide membranes with carboxyl, hydroxyl, and epoxy termination prepared by a post-treatment of Hummers-derived GO indicates that modification with carboxyl groups leads to an increase of the membrane permeance by 30%. At the same time, modification with epoxy groups leads to suppressing membrane permeance by 20%. It is important to note that a variation of terminal groups results in changing the interlayer distance, which is equal to 0.89 nm (1.51 nm), 0.884 nm (1.40 nm), and 0.87 nm (1.32 nm) in the dry (and wet) state for carboxyl, hydroxyl, and epoxy-terminated graphene oxide, respectively. Also, the chemical composition of graphene oxide is tuned by changing the oxidizer activity during the synthesis. The GO suspensions with nearly

Table 1 Influence of microstructural and chemical characteristics of graphene oxide on the membrane performance.

GO properties	Process type	Influence on membrane characteristics		Requirements for controlling the properties
		Permeance	Selectivity	
Interlayer spacing	Gas separation	Moderate	Moderate	– Cross-linking of GO nanosheets in the membrane preparation stage by cations or organic linkers
	Gas dehumidification	Significant	Moderate	
	Liquid separation	Moderate	Significant	– Post mortem GO reduction
				– Application of external pressure
Size of GO nanosheets	All separation processes	Medium degree of influence	Negligible	– Selection of better graphite precursors with appropriate initial microstructure
				– Ultrasonic GO post-treatment
Defects density in GO nanosheets	Gas separation	Significant	Significant	– Varying graphite/oxidizer ratio upon the synthesis
	Liquid separation	Significant	Moderate	– GO post-treatment by oxidizers
Chemical composition of GO nanosheets	Liquid separation	Medium degree of influence	Moderate	– Choice of appropriate GO synthetic routes
	Gas separation	Not determined		– Varying graphite/oxidizer ratio during synthesis
				– GO post-treatment using thermal or chemical reduction

constant content of C–O bonds (~37 at%), and varied content of C=O bonds were obtained by changing the temperature at the last stage of the preparation procedure.[85] Thus prepared membranes demonstrate a water flux increase from 50 to 300 l m^{-2} h^{-1} with as soon as carbonyl group content changes from 22 down to 10 at%. A chemical or thermal treatment also decreases the number of oxygen-containing functional groups, especially C=O bonds. However, this process is associated with significant narrowing of the interlayer distance as the main reason for permeation changes. Thus functional groups, that increase specific sorption of penetrating molecules (hydroxyl groups for water as an example), facilitate the membrane permeance.

The influence of the microstructural and chemical characteristics of graphene oxide on the permeance and selectivity of membranes during the implementation of separation processes in gas and liquid media, as well as methods for controlling these properties are summarized in Table 1.

Application of graphene oxide membranes

Gas and vapor separation

The first practical application of a graphene oxide membrane for substance separation was demonstrated by Nair *et al.*[2] A free-standing graphene oxide membrane with a thickness of about 1 micron completely blocks gas molecules and alcohol vapors, whereas it permits ultrafast permeation of water vapors. During the last 8 years, a huge progress has been achieved in using GO membranes for gas separation. All the obtained results are ranged, as polymeric membranes suggest, in two groups – membranes with diffusion (molecular sieving) and the ones with a sorption type of selectivity. Transport through the interlayer galleries into graphene oxide membranes allows them to realize size exclusion, which provides hydrogen or helium permeance 2–3 order of magnitude higher than that for larger molecules (CO_2, N_2, CH_4). Early published results on hydrogen separation using GO membranes are summarized in the Robeson plot – typical graph for demonstrating correlations between membrane permeability and selectivity (Figure 7). One can see that utilization of graphene oxide allows for breaking through permeability–selectivity trade-off characteristic for polymers.[86]

On the other hand, graphene oxide, due to its hydrophilic nature and specific oxygen-containing groups, demonstrates the sorption type of selectivity. As an example, GO membranes demonstrating CO_2/N_2 selectivity over 670 are prepared.[87,88] However, outstanding results are obtained in the field of gas dehumidification using the GO membranes. Membranes with water permeability exceeding 10^5 Barrer and H_2O/N_2 selectivity over 10^4 at relative humidity ~80% were produced.[12,89] These

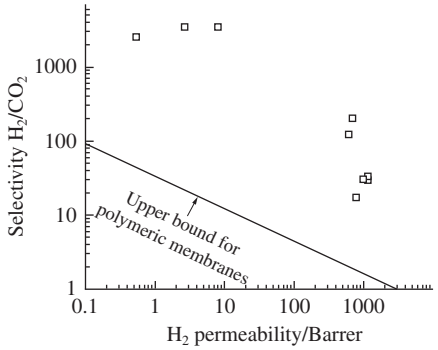

Figure 7 Comparison of graphene oxide based membranes hydrogen permeability and selectivity in pair H_2/CO_2 with upper bound for polymeric membranes, the data are obtained elsewhere.[53]

characteristics allow one to utilize graphene oxide based membranes for industrial gas and air dehumidification.

Pervaporation

The anomalous water transport through the laminated graphene oxide membranes also promises a great opportunity for their utilization in pervaporation processes. Pervaporation is known as a method for separation liquid mixtures by partial vaporization of the required component through the membrane. The graphene oxide membranes are applied to selective removing water from alcohol–water mixtures to prepare concentrated alcohols, such as ethanol, isopropanol, or butanol.[43,90–94] The trade-off between the water–alcohol separation factor and the water flux through the membrane for graphene-oxide and cross-linked graphene

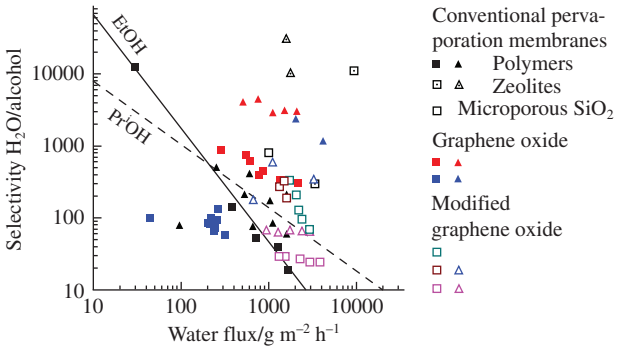

Figure 8 Permeance–selectivity trade-off for graphene oxide based membranes and conventional polymeric and zeolite membranes in pervaporation separation of alcohol–water mixtures. The squares symbols indicate the data for H_2O/EtOH separation, triangles correspond to H_2O/PrⁱOH separation, the data for initial graphene oxide membranes are taken elsewhere,[90,96,97] modified graphene oxide membranes are described in refs. 91–93, conventional pervaporation membranes are given in ref. 98.

oxide membranes and polymeric and also zeolite membranes (used as a reference) is shown in Figure 8. The properties of graphene oxide based membranes are superior to those of polymeric materials and are comparable to those of membranes based on microporous silica. However, membranes based on zeolite-A and zeolite-Z demonstrate a better performance than the GO membranes. Simultaneously, the preparation of defect-free zeolite membranes is a much more time-consuming and expensive process than the preparation of laminated GO membranes. Long term stability is assumed as the main problem of GO membranes. However, the cross-linking approach makes it possible to stabilize membranes, demonstrating performance for *ca*. 120 h.[95]

Water desalination

Pressure-driven water purification processes include, as known, microfiltration, ultrafiltration, nanofiltration, and reverse osmosis. Owing to the size of interlayer galleries available for molecular transport, less than 1 nm GO membranes can be utilized in the last two above mentioned processes being effective for removing small organic molecules and inorganic salts from solution. For example, graphene oxide membranes demonstrate near-complete rejection (>95%) for small organic dyes with a reasonable water permeance of ~10–40 l m^{-2} bar^{-1} h^{-1}.[46,74] In the case of water desalination, salt rejection's efficiency strongly depends on the anion and cation charge. According to the Donnan exclusion theory, the negatively charged GO nanosheets repel cations and retain anions to keep the electroneutrality. As predicted by the Donnan exclusion theory, GO membranes demonstrate the highest rejection for 1–2 electrolyte (Na_2SO_4 rejection ~63%) and the lowest rejection for 2–1 electrolyte ($MgCl_2$ rejection ~15%). For the same valence ratio of the negatively charged and positively charged ions, the rejection of $MgSO_4$ (42%) is higher than the NaCl rejection (28%) due to the larger hydrated radius both for Mg^{2+} (0.43 nm) and SO_4^{2-} (0.38 nm) compared to those for Na^+ (0.36 nm) and Cl^- (0.33 nm).[99] The main problem during such liquid separation processes is found to be the GO layer swelling leading to an abrupt decrease of rejection characteristics and even to the membrane damage. Several techniques, such as cross-linking,[100] partial reduction,[80] and external pressure regulation,[11] allow one to overcome this problem. These approaches make it possible to form stable GO membranes with suitable permeance–rejection characteristics. We summarize early published data for water permeance and NaCl rejection for different GO membranes (Figure 9), also the obtained data were compared with widely utilized polymeric reverse osmosis and nanofiltration membranes.[101] One can see that careful tuning membrane parameters/separation conditions allows highly effective desalination membranes to be prepared.

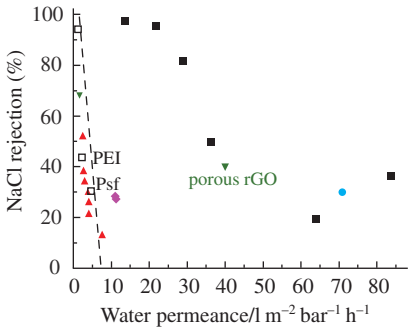

Figure 9 Permeance–rejection trade-off for graphene oxide based membranes and conventional polymeric and zeolite membranes in desalination of NaCl solution. Data obtained from refs. 11 (■), 102 (▲), 80 (▼), 46 (●), 99 (◆) and 101 (□).

Smart and switchable membranes based on graphene oxide

The possibility to control membrane permeance or selectivity by external stimuli allows one to tune the process directly in membrane setup without termination of their ongoing operation, so the development of such smart membranes is of practical interest.[103] A significant progress in polymer chemistry allows for preparing polymeric materials, which response to the solution pH or presence of different species, pressure or temperature of separation process or applying electric, magnetic or electromagnetic field.[104] From the above analysis, it is obvious that graphene oxide might be suggested as a perfect platform for creation of smart and switchable membranes owing to the possibility of *d*-spacing variation to tune membrane permeance and selectivity. However, according to the literature analysis, only a few works are devoted at present to fabrication of graphene oxide switchable membranes.

Introducing photoresponse compounds like [1-(2-hydroxyethyl)-3,3-dimethylindolino-6′-nitrobenzopyrylospiran] into graphene oxide interlayer space allows one to fabricate membrane-scale 2D nanofluidic diodes which can reversibly and rapidly switch between high- and low-rectifying states with ionic current rectification ratio of about 50.[105] Grafting graphene oxide with poly(*N*-isopropylacrylamide) enables one to prepare membranes with reversible positive/negative gating regularity depending on grafting density. Thus, water and small molecule permeance of the membranes can be regulated simply by the adjusting of environment temperature. At low grafting density, a temperature increase from 25 to 50 °C leads to water permeance growth from 15 to 30 l m^{-2} bar^{-1} h^{-1} associated with Rodamine B rejection decreasing from 95 to 85%. At high grafting density, a temperature increase suppresses membrane permeance from 15 to 3 l m^{-2} bar^{-1} h^{-1} associated with Rodamine B rejection growth from 73 to 100%.[106] Introduction of CO_2-responsive polymer, poly(*N*,*N*-dimethylaminoethyl methacrylate) into graphene oxide allows one to fabricate CO_2-responsive membrane. Membrane immersing in CO_2-containg solution for 30 min leads to reversible suppressing the water permeance from 50 to 153 l m^{-2} bar^{-1} h^{-1} associated with growth of $MgCl_2$ from 5 to 45%.[107]

The switching behavior in the discussed cases is determined by the properties of organic molecules introduced between GO nanosheets. At the same time, utilization of intrinsic properties of graphene oxide for preparation of switchable membranes was discussed only in one early published work.[108] In this work, an electrical control over water permeation through the graphene oxide membranes with preliminary formed conductive filaments by controllable electrical breakthrough was accomplished. The analogous approach was discussed for the formation of memristive elements.[109,110] Applications of 20 mA current to Ag/GO/Au structure leads to suppressing a water permeation rate by a factor of 14 due to controllable ionization of water molecules in the interlayer galleries. A sketch illustrating the main mechanisms of switching graphene oxide based membranes is shown in Figure 10.

Conclusions and perspectives

A lot of studies have demonstrated the extraordinary performance of laminar graphene oxide membranes in different separation processes. The membranes demonstrate extraordinary water permeance and excellent gas separation properties (especially for small molecules) that overcome the limited performance of widely utilized polymeric membranes. A detailed analysis of gas transport mechanism indicates that the interlayer distance is a crucial factor determining both membrane permeance and selectivity. Also, the presence of defects and different functions have a high impact on the membrane performance.

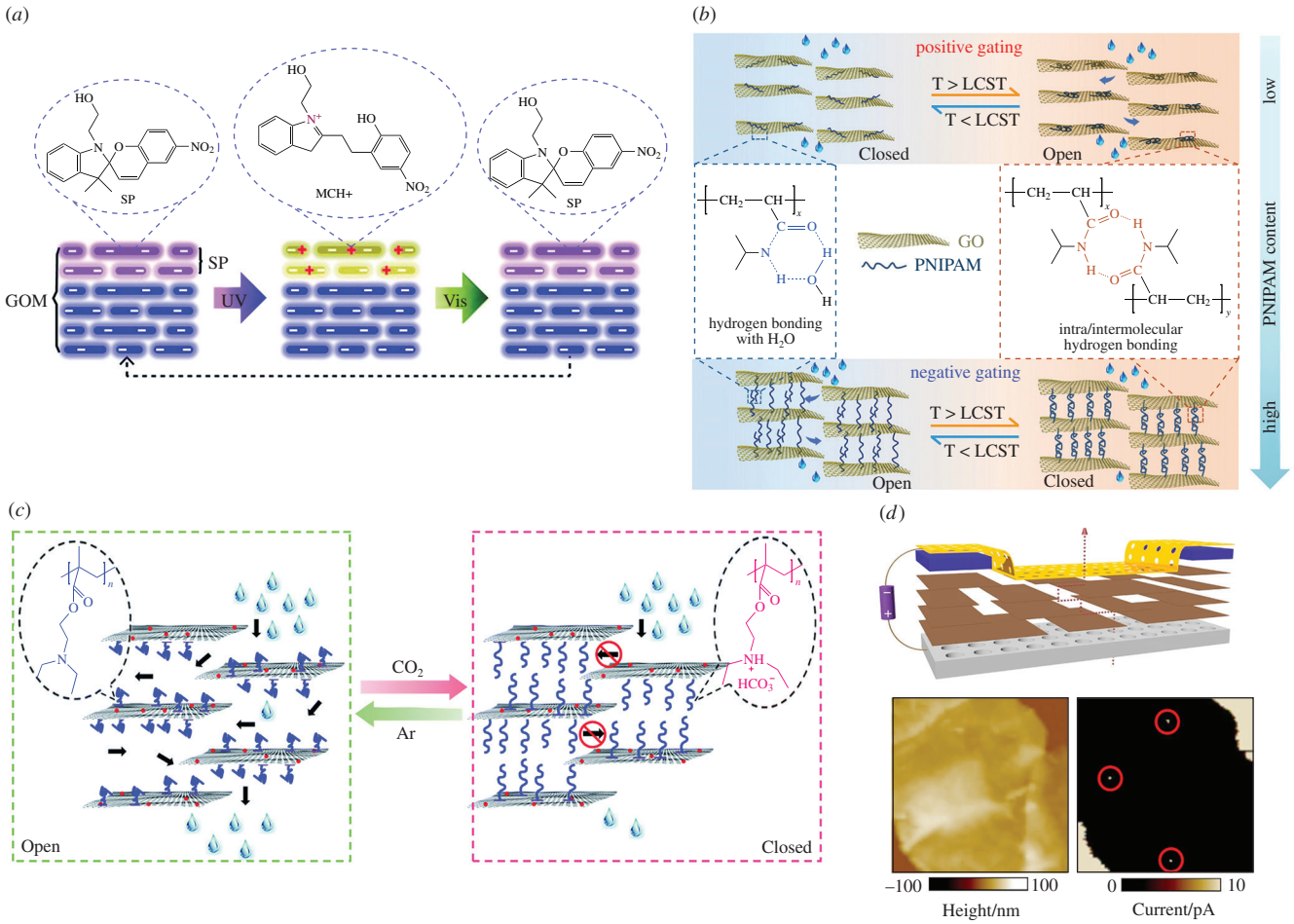

Figure 10 Scheme illustrating principles of performance of graphene oxide based (*a*) photoresponse membrane (reproduced from ref. 105 with permission from the Royal Society of Chemistry), (*b*) thermoresponse membrane (reproduced from ref. 106 with permission from Wiley), (*c*) CO_2-response membrane (reproduced from ref. 107 with permission from the Royal Society of Chemistry) and (*d*) electrically-switchable membranes (reproduced from ref. 108 with permission from Springer Nature).

Despite the significant progress achieved in the preparation and study of GO membranes, several problems and challenges should be solved for the wide utilization of graphene oxide membranes in membrane technology. First of all, synthetic procedures for more effective and low-cost production of graphene oxide suspensions with controlled physico-chemical properties, including a nanosheets lateral size, the number of in-plane defects and functional groups, should be developed. The preparation techniques for fabrication of defect-free ideally packed GO membranes on different large area substrates, including tubular and hollow-fiber porous membranes, should be developed. Also, for practical applications of the GO membranes, new efforts should be taken toward the improvement of their long-term stability and development of approaches for suppressing swelling and other degradation processes. Several promising strategies such as chemical cross-linking or physical confinement, would be suggested for this purpose. Finally, a more accurate model of substance transport should be proposed for the correct description of transport properties of the GO membranes. *In situ* and *in operando* characterization techniques, combined with simulation results, should be advanced to understand membrane performance and the restrictions in their practical use. It should be also noted that MAXEN materials and membranes are being intensively developed in parallel to the GO membranes, and this competition is technologically beneficial and pushes up new ideas and technologically relevant solutions for both the competitors.[111–113] We hope that the complex investigation and modeling of separation processes in the field of graphene oxide membranes by the scientific community and engineers will allow them to integrate membranes into technologically important processes rather quickly.

This review is supported by RFBR (grant no. 18-29-19120). The authors are grateful to A. A. Eliseev and M. V. Korobov for fruitful discussions. D. I. Petukhov is also thankful to the Russian Science Foundation (grant no. 20-79-10205) for financial support in the part of literature assay devoted to graphene oxide membranes preparation techniques and smart membranes based on graphene oxide. This research has been supported by the Interdisciplinary Scientific and Educational School of M. V. Lomonosov Moscow State University ‘Future Planet and Global Environmental Change’.

References

1 K. S. Novoselov, V. I. Fal’ko, L. Colombo, P. R. Gellert, M. G. Schwab and K. Kim, *Nature*, 2012, **490**, 192.
2 R. R. Nair, H. A. Wu, P. N. Jayaram, I. V Grigorieva and A. K. Geim, *Science*, 2012, **335**, 442.
3 L. Zhang and M. Jaroniec, *Chem. Soc. Rev.*, 2020, **49**, 6039.
4 Y. Cheng, Y. Pu and D. Zhao, *Chem. – Asian J.*, 2020, **15**, 2241.
5 E. Yang, M.-H. Ham, H. B. Park, C.-M. Kim, J. Song and I. S. Kim, *J. Membr. Sci.*, 2018, **547**, 73.
6 T. Mizoguchi, M. Honda, S. Ida and M. Koinuma, *Chem. Lett.*, 2020, **49**, 376.
7 D. R. Dreyer, S. Park, C. W. Bielawski and R. S. Ruoff, *Chem. Soc. Rev.*, 2010, **39**, 228.
8 A. Yu. Romanchuk, A. S. Slesarev, S. N. Kalmykov, D. V Kosynkin and J. M. Tour, *Phys. Chem. Chem. Phys.*, 2013, **15**, 2321.
9 F. Liu, C. Wang, X. Sui, M. A. Riaz, M. Xu, L. Wei and Y. Chen, *Carbon Energy*, 2019, **1**, 173.

10 H. Li, Z. Song, X. Zhang, Y. Huang, S. Li, Y. Mao, H. J. Ploehn, Y. Bao and M. Yu, *Science*, 2013, **342**, 95.
11 W. Li, W. Wu and Z. Li, *ACS Nano*, 2018, **12**, 9309.
12 D. I. Petukhov, E. A. Chernova, O. O. Kapitanova, O. V. Boytsova, R. G. Valeev, A. P. Chumakov, O. V. Konovalov and A. A. Eliseev, *J. Membr. Sci.*, 2019, **577**, 184.
13 O. O. Kapitanova, E. Yu. Kataev, D. Yu. Usachov, A. P. Sirotina, A. I. Belova, H. Sezen, M. Amati, M. Al-Hada, L. Gregoratti, A. Barinov, H. D. Cho, T. W. Kang, G. N. Panin, D. Vyalikh, D. M. Itkis and L. V. Yashina, *J. Phys. Chem. C*, 2017, **121**, 27915.
14 I. Childres, L. A. Jauregui, J. Tian and Y. P. Chen, *New J. Phys.*, 2011, **13**, 25008.
15 Y. Mulyana, M. Uenuma, Y. Ishikawa and Y. Uraoka, *J. Phys. Chem. C*, 2014, **118**, 27372.
16 S. C. O'Hern, M. S. H. Boutilier, J.-C. Idrobo, Y. Song, J. Kong, T. Laoui, M. Atieh and R. Karnik, *Nano Lett.*, 2014, **14**, 1234.
17 B. C. Brodie, *Philos. Trans. R. Soc. London*, 1859, **149**, 249.
18 L. Staudenmaier, *Ber. Dtsch. Chem. Ges*., 1898, **31**, 1481.
19 W. S. Hummers and R. E. Offeman, *J. Am. Chem. Soc.*, 1958, **80**, 1339.
20 K. Krishnamoorthy, M. Veerapandian, K. Yun and S.-J. Kim, *Carbon*, 2013, **53**, 38.
21 J. Chen, Y. Zhang, M. Zhang, B. Yao, Y. Li, L. Huang, C. Li and G. Shi, *Chem. Sci.*, 2016, **7**, 1874.
22 Y. Ying, L. Sun, Q. Wang, Z. Fan and X. Peng, *RSC Adv.*, 2014, **4**, 21425.
23 Y. Gao, Y. He, S. Yan, H. Yu, J. Ma, R. Hou, Y. Fan and X. Yin, *J. Mater. Sci.*, 2020, **55**, 15130.
24 A. V. Talyzin, A. Klechikov, M. Korobov, A. T. Rebrikova, N. V. Avramenko, M. F. Gholami, N. Severin and J. P. Rabe, *Nanoscale*, 2015, **7**, 12625.
25 A. Talyzin, G. Mercier, A. Klechikov, M. Hedenström, D. Johnels, D. Wei, D. Cotton, A. Opitz and E. Moons, *Carbon*, 2017, **115**, 430.
26 D. C. Marcano, D. V. Kosynkin, J. M. Berlin, A. Sinitskii, Z. Sun, A. Slesarev, L. B. Alemany, W. Lu and J. M. Tour, *ACS Nano*, 2010, **4**, 4806.
27 D. I. Petukhov, E. A. Chernova, O. O. Kapitanova, O. V. Boytsova, R. G. Valeev, A. P. Chumakov, O. V. Konovalov and A. A. Eliseev, *J. Membr. Sci.*, 2019, **577**, 184.
28 K. N. Kudin, B. Ozbas, H. C. Schniepp, R. K. Prud'homme, I. A. Aksay and R. Car, *Nano Lett.*, 2008, **8**, 36.
29 L. Dong, J. Yang, M. Chhowalla and K. P. Loh, *Chem. Soc. Rev.*, 2017, **46**, 7306.
30 S. H. Aboutalebi, M. M. Gudarzi, Q. B. Zheng and J.-K. Kim, *Adv. Funct. Mater.*, 2011, **21**, 2978.
31 S. Pan and I. A. Aksay, *ACS Nano*, 2011, **5**, 4073.
32 C. Cai, N. Sang, Z. Shen and X. Zhao, *J. Exp. Nanosci.*, 2017, **12**, 247.
33 P. Yu, S. E. Lowe, G. P. Simon and Y. L. Zhong, *Curr. Opin. Colloid Interface Sci.*, 2015, **20**, 329.
34 C.-Y. Yang, C.-L. Wu, Y.-H. Lin, L.-H. Tsai, Y.-C. Chi, J.-H. Chang, C.-I. Wu, H.-K. Tsai, D.-P. Tsai and G.-R. Lin, *Opt. Mater. Express*, 2013, **3**, 1893.
35 P. P. Brisebois and M. Siaj, *J. Mater. Chem. C*, 2020, **8**, 1517.
36 D. Cohen-Tanugi and J. C. Grossman, *Nano Lett.*, 2014, **14**, 6171.
37 L. Wang, M. S. H. Boutilier, P. R. Kidambi, D. Jang, N. G. Hadjiconstantinou and R. Karnik, *Nat. Nanotechnol.*, 2017, **12**, 509.
38 L.-C. Lin and J. C. Grossman, *Nat. Commun.*, 2015, **6**, 8335.
39 C. Athanasekou, M. Pedrosa, T. Tsoufis, L. M. Pastrana-Martínez, G. Romanos, E. Favvas, F. Katsaros, A. Mitropoulos, V. Psycharis and A. M. T. Silva, *J. Membr. Sci.*, 2017, **522**, 303.
40 J. Zhao, Y. Zhu, G. He, R. Xing, F. Pan, Z. Jiang, P. Zhang, X. Cao and B. Wang, *ACS Appl. Mater. Interfaces*, 2016, **8**, 2097.
41 Q. Xin, F. Ma, L. Zhang, S. Wang, Y. Li, H. Ye, X. Ding, L. Lin, Y. Zhang and X. Cao, *J. Membr. Sci.*, 2019, **586**, 23.
42 X. Li, L. Ma, H. Zhang, S. Wang, Z. Jiang, R. Guo, H. Wu, X. Cao, J. Yang and B. Wang, *J. Membr. Sci.*, 2015, **479**, 1.
43 C.-H. Tsou, Q.-F. An, S.-C. Lo, M. De Guzman, W.-S. Hung, C.-C. Hu, K.-R. Lee and J.-Y. Lai, *J. Membr. Sci.*, 2015, **477**, 93.
44 J. Zhu, X. Meng, J. Zhao, Y. Jin, N. Yang, S. Zhang, J. Sunarso and S. Liu, *J. Membr. Sci.*, 2017, **535**, 143.
45 M. Fathizadeh, H. N. Tien, K. Khivantsev, J.-T. Chen and M. Yu, *J. Mater. Chem. A*, 2017, **5**, 20860.
46 A. Akbari, P. Sheath, S. T. Martin, D. B. Shinde, M. Shaibani, P. C. Banerjee, R. Tkacz, D. Bhattacharyya and M. Majumder, *Nat. Commun.*, 2016, **7**, 10891.
47 H. W. Kim, H. W. Yoon, B. M. Yoo, J. S. Park, K. L. Gleason, B. D. Freeman and H. B. Park, *Chem. Commun.*, 2014, **50**, 13563.
48 A. F. M. Ibrahim and Y. S. Lin, *Chem. Eng. Sci.*, 2018, **190**, 312.
49 B. Qi, X. He, G. Zeng, Y. Pan, G. Li, G. Liu, Y. Zhang, W. Chen and Y. Sun, *Nat. Commun.*, 2017, **8**, 825.
50 H. Liu, S. Li, D. Sun, Y. Chen, Y. Zhou and T. Lu, *J. Mater. Chem. B*, 2014, **2**, 2212.
51 W. Choi, J. Choi, J. Bang and J.-H. Lee, *ACS Appl. Mater. Interfaces*, 2013, **5**, 12510.
52 M. Wang, L.D. Duong, J.-S. Oh, N. T. Mai, S. Kim, S. Hong, T. Hwang, Y. Lee and J.-D. Nam, *ACS Appl. Mater. Interfaces*, 2014, **6**, 1747.
53 A. Ibrahim and J. Lin, *J. Membr. Sci.*, 2018, **550**, 238.
54 S. Zheng, Q. Tu, J. J. Urban, S. Li and B. Mi, *ACS Nano*, 2017, **11**, 6440.
55 K. Guan, J. Shen, G. Liu, J. Zhao, H. Zhou and W. Jin, *Sep. Purif. Technol.*, 2017, **174**, 126.
56 A. A. Eliseev, A. S. Kumskov, N. S. Falaleev, V. G. Zhigalina, A. A. Eliseev, A. A. Mitrofanov, D. I. Petukhov, A. L. Vasiliev and N. A. Kiselev, *J. Phys. Chem. C*, 2017, **121**, 23669.
57 Y. Jin, Y. Fan, X. Meng, W. Zhang, B. Meng, N. Yang and S. Liu, *Processes*, 2019, **7**, 751.
58 V. Levdansky, O. Šolcová, K. Friess and P. Izák, *Appl. Sci.*, 2020, **10**, 455.
59 D. I. Petukhov and A. A. Eliseev, *Nanotechnology*, 2016, **27**, 085707.
60 D. Petukhov, I. Sadilov, R. Vasiliev, L. Kozina and A. Eliseev, *J. Mater. Chem. A*, 2019, **7**, 21684.
61 D. I. Petukhov, A. S. Kan, A. P. Chumakov, O. V. Konovalov, R. G. Valeev and A. A. Eliseev, *J. Membr. Sci.*, 2021, **621**, 118994.
62 H. Yoshida and L. Bocquet, *J. Chem. Phys.*, 2016, **144**, 234701.
63 D. I. Petukhov, M. V. Berekchiian, E. S. Pyatkov, K. A. Solntsev and A. A. Eliseev, *J. Phys. Chem. C*, 2016, **120**, 10982.
64 A. A. Eliseev, A. A. Poyarkov, E. A. Chernova, A. A. Eliseev, A. P. Chumakov, O. V. Konovalov and D. I. Petukhov, *2D Mater.*, 2019, **6**, 035039.
65 A. Iakunkov, J. Sun, A. Rebrikova, M. Korobov, A. Klechikov, A. Vorobiev, N. Boulanger and A. V. Talyzin, *J. Mater. Chem. A*, 2019, **7**, 11331.
66 A. Klechikov, J. Sun, A. Vorobiev and A. V. Talyzin, *J. Phys. Chem. C*, 2018, **122**, 13106.
67 M. V. Korobov, A. V. Talyzin, A. T. Rebrikova, E. A. Shilayeva, N. V. Avramenko, A. N. Gagarin and N. B. Ferapontov, *Carbon*, 2016, **102**, 297.
68 T. Daio, T. Bayer, T. Ikuta, T. Nishiyama, K. Takahashi, Y. Takata, K. Sasaki and S. M. Lyth, *Sci. Rep.*, 2015, **5**, 11807.
69 E. A. Chernova, D. I. Petukhov, O. O. Kapitanova, O. V. Boytsova, A. V. Lukashin and A. A. Eliseev, *Nanosyst.: Phys., Chem., Math.*, 2018, **9**, 614.
70 A. Klechikov, J. Sun, I. A. Baburin, G. Seifert, A. T. Rebrikova, N. V. Avramenko, M. V. Korobov and A. V. Talyzin, *Nanoscale*, 2017, **9**, 6929.
71 A. V. Talyzin, T. Hausmaninger, S. You and T. Szabo, *Nanoscale*, 2014, **6**, 272.
72 S. You, J. Yu, B. Sundqvist, L. A. Belyaeva, N. V. Avramenko, M. V. Korobov and A. V. Talyzin, *J. Phys. Chem. C*, 2013, **117**, 1963.
73 Z. Wang, F. He, J. Guo, S. Peng, X. Q. Cheng, Y. Zhang, E. Drioli, A. Figoli, Y. Li and L. Shao, *Mater. Adv.*, 2020, **1**, 554.
74 M. Zhang, Y. Mao, G. Liu, G. Liu, Y. Fan and W. Jin, *Angew. Chem., Int. Ed.*, 2020, **59**, 1689.
75 L. Chen, G. Shi, J. Shen, B. Peng, B. Zhang, Y. Wang, F. Bian, J. Wang, D. Li, Z. Qian, G. Xu, G. Liu, J. Zeng, L. Zhang, Y. Yang, G. Zhou, M. Wu, W. Jin, J. Li and H. Fang, *Nature*, 2017, **550**, 380.
76 Z. Li, Y. Xing, X. Fan, L. Lin, A. Meng and Q. Li, *Desalination*, 2018, **443**, 130.
77 J. S. Roh, T. H. Choi, T. H. Lee, H. W. Yoon, J. Kim, H. W. Kim and H. B. Park, *J. Phys. Chem. Lett.*, 2019, **10**, 7725.
78 A. F. M. Ibrahim, F. Banihashemi and Y. S. Lin, *Chem. Commun.*, 2019, **55**, 3077.
79 L. Nie, K. Goh, Y. Wang, J. Lee, Y. Huang, H. E. Karahan, K. Zhou, M. D. Guiver and T.-H. Bae, *Sci. Adv.*, 2020, **6**, eaaz9184.
80 Y. Li, W. Zhao, M. Weyland, S. Yuan, Y. Xia, H. Liu, M. Jian, J. Yang, C. D. Easton, C. Selomulya and X. Zhang, *Environ. Sci. Technol.*, 2019, **53**, 8314.
81 R. Qiu, J. Xiao, X. D. Chen, C. Selomulya, X. Zhang and M. W. Woo, *ACS Appl. Mater. Interfaces*, 2020, **12**, 4769.
82 F. Mouhat, F.-X. Coudert and M.-L. Bocquet, *Nat. Commun.*, 2020, **11**, 1566.
83 C. Chen, L. Jia, J. Li, L. Zhang, L. Liang, E. Chen, Z. Kong, X. Wang, W. Zhang and J.-W. Shen, *Desalination*, 2020, **491**, 114560.

84 B. Chen, H. Jiang, X. Liu and X. Hu, *Phys. Chem. Chem. Phys.*, 2018, **20**, 9780.
85 S. Kumar, A. Garg and A. Chowdhuri, *Mater. Res. Express*, 2018, **6**, 15604.
86 C. Y. Chuah, J. Lee and T.-H. Bae, *Membranes (Basel)*, 2020, **10**, 336.
87 F. Zhou, H. N. Tien, W. L. Xu, J.-T. Chen, Q. Liu, E. Hicks, M. Fathizadeh, S. Li and M. Yu, *Nat. Commun.*, 2017, **8**, 2107.
88 A. Ali, R. Pothu, S. H. Siyal, S. Phulpoto, M. Sajjad and K. H. Thebo, *Mater. Sci. Energy Technol.*, 2019, **2**, 83.
89 Y. Shin, W. Liu, B. Schwenzer, S. Manandhar, D. Chase-Woods, M. H. Engelhard, R. Devanathan, L. S. Fifield, W. D. Bennett, B. Ginovska and D. W. Gotthold, *Carbon*, 2016, **106**, 164.
90 G. Li, L. Shi, G. Zeng, Y. Zhang and Y. Sun, *RSC Adv.*, 2014, **4**, 52012.
91 J. Zhao, Y. Zhu, F. Pan, G. He, C. Fang, K. Cao, R. Xing and Z. Jiang, *J. Membr. Sci.*, 2015, **487**, 162.
92 G. Liu, Z. Jiang, C. Chen, L. Hou, B. Gao, H. Yang, H. Wu, F. Pan, P. Zhang and X. Cao, *J. Membr. Sci.*, 2017, **537**, 229.
93 E. Halakoo and X. Feng, *Chem. Eng. Sci.*, 2020, **216**, 115488.
94 M. B. M. Y. Ang, M. R. Gallardo, G. V. C. Dizon, M. R. De Guzman, L. L. Tayo, S.-H. Huang, C.-L. Lai, H.-A. Tsai, W.-S. Hung, C.-C. Hu, Y. Chang and K.-R. Lee, *J. Membr. Sci.*, 2019, **587**, 117188.
95 W.-S. Hung, C.-H. Tsou, M. De Guzman, Q.-F. An, Y.-L. Liu, Y.-M. Zhang, C.-C. Hu, K.-R. Lee and J.-Y. Lai, *Chem. Mater.*, 2014, **26**, 2983.
96 T.-M. Yeh, Z. Wang, D. Mahajan, B. S. Hsiao and B. Chu, *J. Mater. Chem. A*, 2013, **1**, 12998.
97 W.-S. Hung, Q.-F. An, M. De Guzman, H.-Y. Lin, S.-H. Huang, W.-R. Liu, C.-C. Hu, K.-R. Lee and J.-Y. Lai, *Carbon*, 2014, **68**, 670.
98 P. D. Chapman, T. Oliveira, A. G. Livingston and K. Li, *J. Membr. Sci.*, 2008, **318**, 5.
99 L. Chen, J.-H. Moon, X. Ma, L. Zhang, Q. Chen, L. Chen, R. Peng, P. Si, J. Feng, Y. Li, J. Lou and L. Ci, *Carbon*, 2018, **130**, 487.
100 J. Su, M. Jia, W. Wu, Z. Li and W. Li, *Environ. Sci. Nano*, 2020, **7**, 2924.
101 N. Song, X. Gao, Z. Ma, X. Wang, Y. Wei and C. Gao, *Desalination*, 2018, **437**, 59.
102 Y. Li, S. Yuan, Y. Xia, W. Zhao, C. D. Easton, C. Selomulya and X. Zhang, *J. Membr. Sci.*, 2020, **601**, 117900.
103 W. Lee, D. Kim, S. Lee, J. Park, S. Oh, G. Kim, J. Lim and J. Kim, *Nano Today*, 2018, **23**, 97.
104 S. Darvishmanesh, X. Qian and S. R. Wickramasinghe, *Curr. Opin. Chem. Eng.*, 2015, **8**, 98.
105 L. Wang, Y. Feng, Y. Zhou, M. Jia, G. Wang, W. Guo and L. Jiang, *Chem. Sci.*, 2017, **8**, 4381.
106 J. Liu, L.-J. Yu, G. Yue, N. Wang, Z. Cui, L. Hou, J. Li, Q. Li, A. Karton, Q. Cheng, L. Jiang and Y. Zhao, *Adv. Funct. Mater.*, 2019, **29**, 1808501.
107 L. Dong, W. Fan, X. Tong, H. Zhang, M. Chen and Y. Zhao, *J. Mater. Chem. A*, 2018, **6**, 6785.
108 K.-G. Zhou, K. S. Vasu, C. T. Cherian, M. Neek-Amal, J. C. Zhang, H. Ghorbanfekr-Kalashami, K. Huang, O. P. Marshall, V. G. Kravets, J. Abraham, Y. Su, A. N. Grigorenko, A. Pratt, A. K. Geim, F. M. Peeters, K. S. Novoselov and R. R. Nair, *Nature*, 2018, **559**, 236.
109 O. O. Kapitanova, E. V. Emelin, S. G. Dorofeev, P. V. Evdokimov, G. N. Panin, Y. Lee and S. Lee, *J. Mater. Sci. Technol.*, 2020, **38**, 237.
110 O. O. Kapitanova, G. N. Panin, H. D. Cho, A. N. Baranov and T. W. Kang, *Nanotechnology*, 2017, **28**, 204005.
111 Y. Gogotsi and B. Anasori, *ACS Nano*, 2019, **13**, 8491.
112 K. Rasool, R. P. Pandey, P. A. Rasheed, S. Buczek, Y. Gogotsi and K. A. Mahmoud, *Mater. Today*, 2019, **30**, 80.
113 L. Agartan, K. Hantanasirisakul, S. Buczek, B. Akuzum, K. A. Mahmoud, B. Anasori, Y. Gogotsi and E. C. Kumbur, *Desalination*, 2020, **477**, 114267.

Received: 28th January 2021; Com. 21/6436